Fifth International Symposium on Marine Propulsors
smp'17, Espoo, Finland, June 2017

FULL-SCALE MEASUREMENTS OF UNDERWATER RADIATED NOISE OF A CATAMARAN RESEARCH VESSEL

Serkan Turkmen[1], Mehmet Atlar[2] , Noriyuki Sasaki[1]
[1]Newcastle University, Newcastle Upon Tyne, UK
[2]University of Strathclyde, UK

ABSTRACT

In the Marine Strategy Framework Directive (MSFD), the European Commission (EC) has set requirements to reduce the impact of the URN level caused by merchant shipping on marine life (Directive 2008/56/EC) and to achieve Good Environmental Status (GES) by 2020. As a result, Underwater Radiated Noise (URN) has been a major area of research interest.

The main purpose of this paper is to present in-situ URN measurements of Newcastle University's Research vessel, The Princess Royal. The URN measurements were supported by on-board measurements, acceleration and pressure pulse above the propeller as well as digital photography above the propellers. The measured URN level was analyzed to gain in-depth knowledge of the contribution of various noise sources. As expected, spectral characteristics of URN were found to change according to the noise sources. The results showed that URN before cavitation inception was mainly contributed by background noise and engine harmonics. The propeller blade harmonics appeared in the URN spectrum when leading edge vortex cavitation occurred. The URN level significantly increased with strong suction side sheet cavitation. Indistinguishable sources were also observed on the noise spectra both before and after the cavitation inception.

Keywords
Underwater radiated noise, full-scale measurements, cavitation, SONIC

1 INTRODUCTION

There have been a number of valuable studies involving the impact of the underwater radiated noise (URN), generated by ships, on marine life. UNR affects acoustic communication among marine mammals and fishes by masking, diverging or causing hearing loss (Richardson et al. 1995, Noise 2003, Codarin et al. 2009, Slabbekoorn et al. 2010).

Major noise sources of shipping are propeller and machinery systems. URN generated by cavitating propeller has been identified as a most dominant source (Ross 1976, Nilsson & Tyvand 1981). Propeller and hull design may reduce the URN level associated with cavitation. However, this is a challenge due to there are several types of cavitation that appear at different operation conditions.(Atlar et al. 2001, Schuiling et al. 2011, Van & Hendrik 2011, Turkmen et al. 2017).

The EU-FP7 collaborative project SONIC that aimed to investigate and mitigate URN, particularly caused by propeller cavitation (SONIC 2012). A series of full scale URN measurements were conducted within the framework of the project. The Newcastle University Research Vessel Princess Royal (PR) was chosen as a target vessel to measure the URN, pressure pulses and hull vibration (see Figure 1). In this paper full scale sea trials, taken in 2015, are presented. The URN level was analysed for the source level at 1m reference distance analysed in 1/3 octave band according to ANSI standard.

Figure 1 The RV Princess Royal

2 SEA TRIAL

The PR is am 18.9m length and 7.3m width catamaran research vessel. The mean draft was 1.86m during the trial. The operation given in Table 1. The vessel had two 602HP main engine and a gearboxes to reduce the engine rpm at a gear ratio 1.75:1. Each demi hull has a 0.75m diameter, five blades fix pitch propeller (Atlar et al. 2013). Note that the vessel has been having new engines, shafts and propellers since 2016.

The trials were conducted took place in Cambois Bay, North-East coast of England. Water depth was approximately 23m deep. The sea surface was calm and the sea bed consists of uniform sandy mud (fine silt).

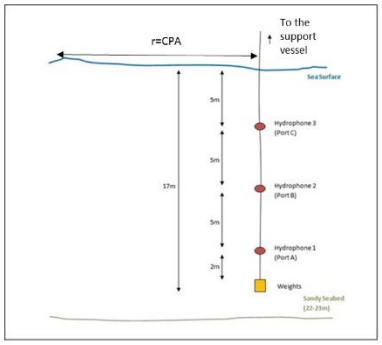

Figure 2 The Hydrophone array deployed from the support vessel

ISO/PAS 17028 and ANSI S12.64 procedures were followed to set the hydrophone array and analyse the data (ISO 2012, ANSI 2009). Three hydrophones, HTI-96-MIN, was deployed by Strathclyde University from a support vessel. Figure 2 shows the deployment configuration.. Although three hydrophones were arranged the measurement procedure was followed for Grade C which requires only one hydrophone. GPS time and position was recorded to define the distance of the Closest Point of Approach (CPA) and data window length (DWL). CPA is the closest distance between the hydrophone array and the target vessel. The vessel should travel a straight line course as drawn in Figure 3 . DWL is the distance covers the start and end data locations. CPA varied from 50m to 3km during the trails however URN was analysed for 50m, 100m and 200m in this study. Pressure pulses were logged with XPM10 Miniature pressure sensors and vibration were logged with B&K 4518-003 accelerometers. The equipment details can be found in Zoet et al. (2015).

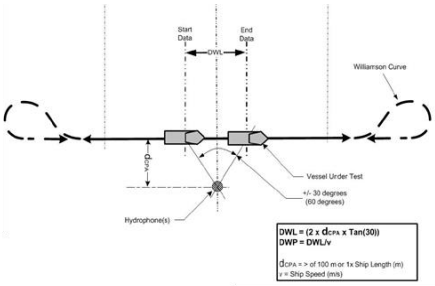

Figure 3 Test course configuration (starboard approaches)

The cavitation observations were made through the PR's Perspex windows where are above each propeller. Still digital images were taken by using Nikon D700 camera with the support of continuous light source.

Table 1 -Full Scale Average Running Conditions

Engine	Nprop	SOG (GPS)
[RPM]	[RPM]	knot
599.9	342.8	4.3
899.5	514	8.1
1189.5	679.5	9.4
1491	852	11.3
1997.625	1141.5	16.3

3 MEASUREMENTS

3.1 URN Measurements

Measured URN data, recorded by hydrophones, is called received sound pressure level (RL). A series of correction is necessary to find the source sound pressure level (SL) of the target vessel. Corrections should include the range, effect of the free surface and seabed.

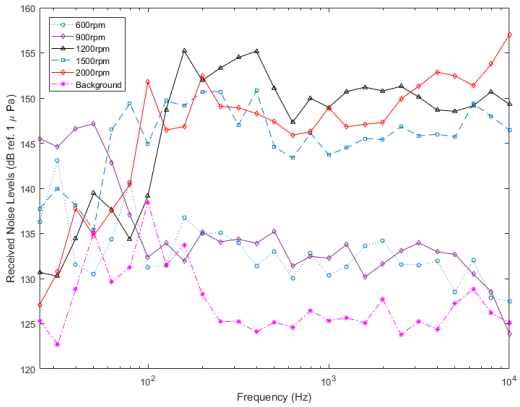

Figure 4 Received noise level (RL) of the vessel (Hydrophone1).

Acoustic intensity of the source reduce with the distance (range) due to the fluid domain. This loss is called as the

transmission loss (TL) or spherical spreading loss is the changes of acoustic intensity and pressure (Urick 1967, Ross 1976). TL is defined as the ratio of r(m), the horizontal distance (r) between the source and the receiver (Closest Point of Approach, CPA), to r_{ref} ,the reference distance defined as 1m due to the fluid domain. The radiated noise level (RNL) is found when the range correction is applied to RL.

$$RNL = RL + 20\log_{10}\left(\frac{r}{r_{ref}}\right) \quad \textbf{1}$$

In Figure 5 and Figure 6 sound spectrograms show the RL is increasing while the vessel passes the hydrophone. It can be also observed that peaks and troughs changes in the frequency spectrum. The reason is that the sound, travelling from the source and radiation of source reflected from the free surface and sea bottom (mirror image) may increase or cancel one another. This effect is generally referred as a Lloyd's Mirror (LM) effect and This pattern is defined as the Lloyd's Mirror Interference Pattern (LMIP) (Urick 1967).

$$LMIP = 10\log_{10}\left(4\sin^2\left(\frac{kd_s d_r}{r}\right)\right) \quad \textbf{2}$$

where k ($2\pi f/c$) is the wavenumber, d_s is the source depth and d_r is the receiver depth. The propellers are 1.15m (ds) under the sea surface. Figure 7 shows the theoretical LMIP plot calculated from the Equation 2 for three hydrophones, depths are given in Figure 7at 50m CPA. The inference field is appearing in the figure as the peaks and troughs. They are disappearing at the frequency range is low and the intensity of the sound decreases as inverse fourth-power spreading in the frequency range between 10 Hz and 1 kHz.

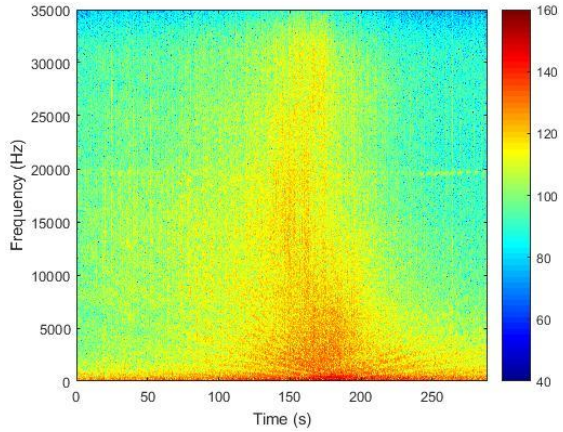

Figure 5 Sound spectrogram of the vessel radiated noise for a pass at 50 m CPA at a speed of 9.4kn (1200rpm) (Hydrophone1).

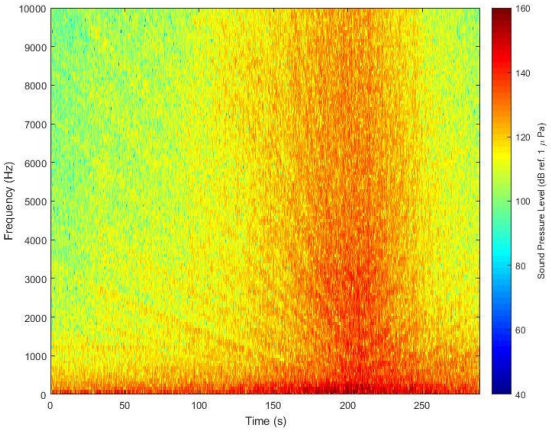

Figure 6 Sound spectrogram of the vessel radiated noise for a pass at 50 m CPA at a speed of 16.3kn (2000rpm) (Hydrophone1).

An incident sound ray, propagating from source to the seabed at grazing angle θ_1, reflects from and transmits through the interface between the fluid and sediment domain as it is demonstrated in Figure 8. The acoustic energy loss (or reflection coefficient, R), associated with reflection from the seabed, is expressed as the ratio of reflected sound intensity (I_r) to incident sound intensity (I_i) (Urick 1967, Ainslie 2010). Conventionally, R is quantify as the logarithmic term bottom reflection loss (BL).

$$R = \frac{I_r}{I_i} \quad \textbf{3}$$

$$BL \equiv -10\log_{10}|R|^2 \quad \textbf{4}$$

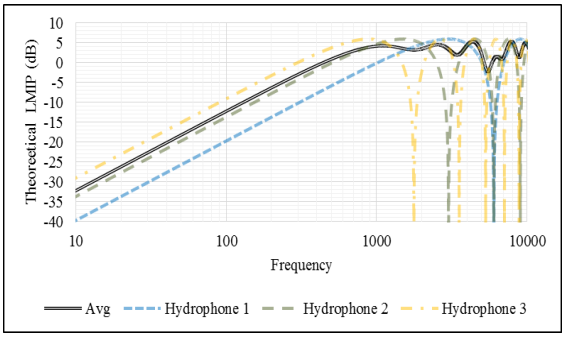

Figure 7 Lloyd's Mirror interference pattern at CPA 50m, source depth 1.15m, d1 5m, d2 10m and d3 17m

A BL model required properties of seabed (i.e., bathymetry and sediment) and water column (i.e., salinity and temperature) properties as well as location of the sources and hydrophones. The sea trail were conducted of a smooth sea bottom consisted of soft mud. The bulk properties of the fluid-sediment interface are given in Table 2. (Ainslie 2010). The maximum and minimum grazing angles are

calculated as 19° and 10°. The incident ray energy can reflect and some amount of its energy can transmit into the sediment layer as shown in Figure 8.

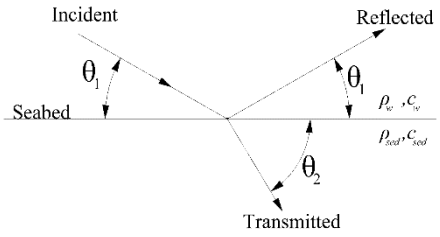

Figure 8 Reflected and transmitted rays at the water-seabed interface

The transmitted ray energy is called transmission coefficient. Transmission coefficient could be contributing factor to the reflection coefficient by reflecting from a boundary at the sediment and substrate. In the present study, the deepest hydrophone measurements were used for 50m of CPA. Therefore, there is no transmitted ray due to the grazing angle is less than a critical angle θ_0. In other words, means total reflection occurs from the seabed (Brekhovskikh 2003).

$$\theta_0 = \arccos\left(\frac{1}{v}\right) \quad \textbf{5}$$

where v is the Sound speed ratio given in Table 2

Table 2 Geo-acoustic parameters of the reflecting boundary

Sediment description	Sound speed ratio (v) C_{sed}/C_w	Density ratio (m)ρ_{sed}/ρ_w	Attenuation coefficient β_{sed} (dB/λ)
Medium silt	1.0479	1.601	0.38

Figure 9shows BL quantified theoretically by using the Rayleigh reflection coefficient(Urick 1967, Ainslie 2010). It should be note that the calculation was made for a single dominant reflection boundary at the fluid-sediment interface. The boundary is perfectly smooth and the critical angle is higher than the grazing angle for any condition.

$$R(\theta) = \frac{\zeta(\theta) - 1}{\zeta(\theta) + 1} \quad \textbf{6}$$

$$\zeta(\theta) = m\frac{tan\theta_1}{tan\theta_2} \quad \textbf{7}$$

θ_2 can be found by using Snell's law and given as a complex angle,

$$\theta_2 = arccos\left(v\frac{cos\theta}{1 + i\varepsilon}\right) \quad \textbf{8}$$

$$\varepsilon = \frac{\log_e 10}{40\pi}\beta_{sed} \quad \textbf{9}$$

where ε is a value function of the sediment attenuation coefficient β_{sed} given in Table 2 at frequencies of 1 kHz or below.

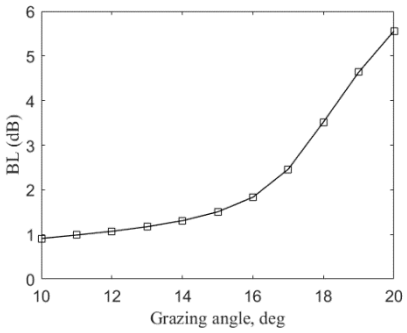

Figure 9 Predicted bottom reflection loss vs. grazing angle

Source level (SL) of the vessel can be calculate by taking into account the corrections.

$$SL^* = RNL - LMIP - BL \quad \textbf{10}$$

The SL of the PR is given in Figure 10.

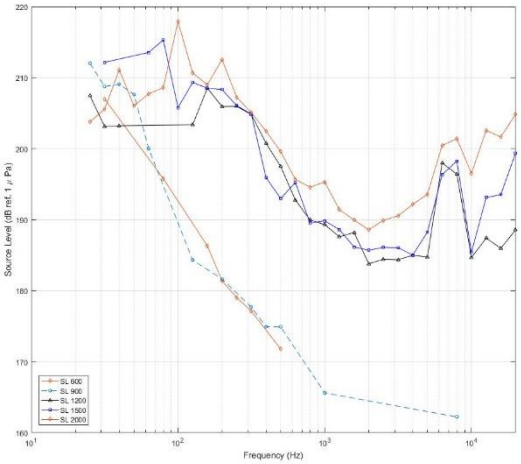

Figure 10 Source level of the vessel

3.2 Cavitation observation

Cavitation appearing on the propeller and its extension are given from low speed to the maximum speed. There is no cavitation observer at 600rpm engine speed (see Figure 11). Irregular leading edge vortex cavitation developed from the suction side of the blade to the rudder at 900 rpm. The sheet cavitation was not significant (see Figure 12). Strong suction side sheet cavitation extending from hub to tip and terminated the blade at 1200 engine speed (see Figure 13). Cloudy sheet cavitation was appearing at 1500 engine speed. The trailing vortex cavitation bursts (see

Figure 14). Heavy tip vortex cavitation and the sheet cavitation was covering almost 25-30% of the suction side of the blade at engine speed 2000 rpm. The Hub-Vortex cavitation is much thicker and the trailing vortex cavitation bursts (see Figure 15). It is also observed irregular propeller-hull vortex cavitation develops at 2000rpm. Further detail of the cavitation observations during the full scale noise trials are given in (Sampson et al. 2015).

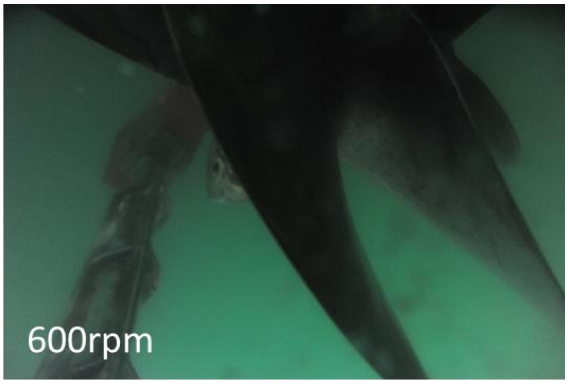

Figure 11 Full-scale trial cavitation observation – 600 engine rpm.

0

Figure 12 Full scale trial cavitation observation– 900 engine rpm.

Figure 13 Full scale trial cavitation observation – 1200 engine rpm

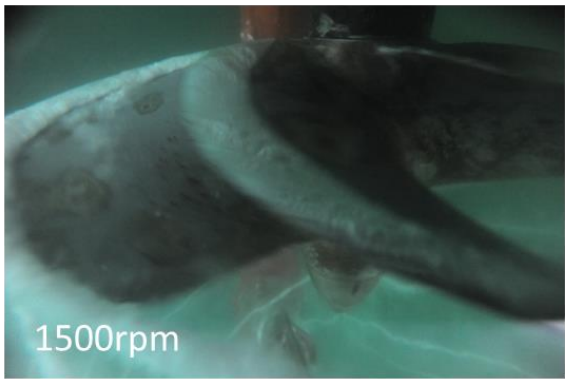

Figure 14 Full scale trial cavitation observation– 1500 engine rpm.

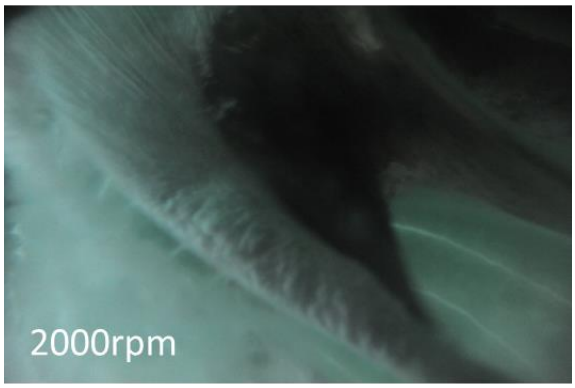

Figure 15 Full scale trial cavitation observation – 2000 engine rpm.

3.3 On-board measurements

Pressure pulses induced by the propeller were measured above and after the propeller from the sensors P2 and P3. The locations of the port side pressure sensors is sketched Figure 16. The results are given in one-third octave band at the frequency range from 10 to 1000Hz where the distinct tones associated with the blade frequencies are develop.

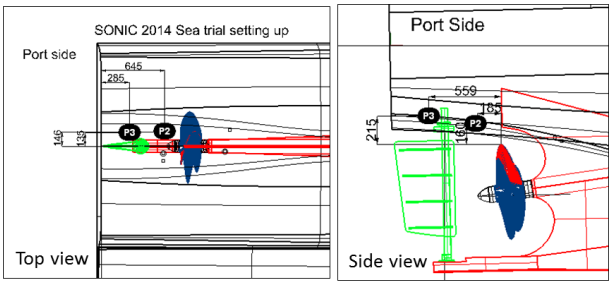

Figure 16 Port side pressure sensors locations

Figure 17 and Figure 18 show that the blade harmonics (BH) are not clear in the non-cavitation and early cavitation stage. Pressure intensities of blade harmonics (BH) are increasing with the propeller speed. One of the significant change of pressure pulses is appeared at the quarter of the first BH at 1500rpm and 2000rpm operation conditions. The reason might be the interaction of the tip vortex, cloud with the sheet cavity. This frequency is also multiples of the propeller shaft rotation frequencies.

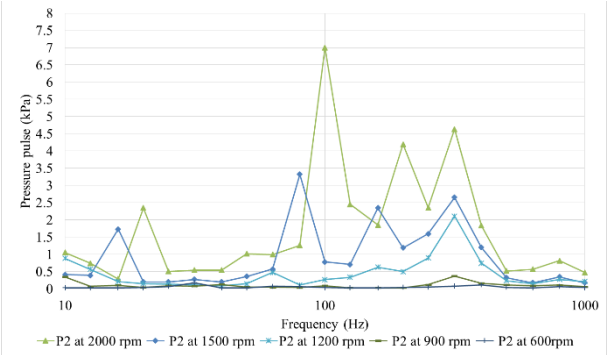

Figure 17 1/3 Octave band pressure pulses on P2.

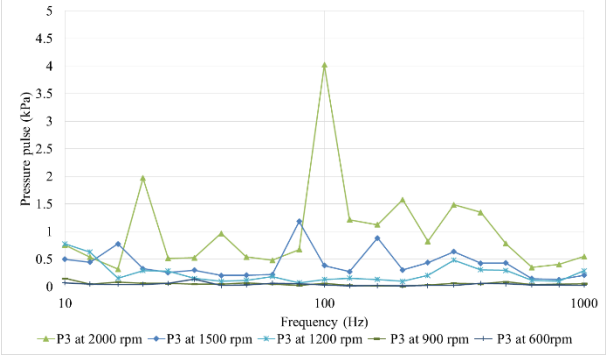

Figure 18 1/3 Octave band pressure pulses on P3.

In Figure 19 the plot of the engine vibrations are presented at 2000rpm. The graph shows the measurements taken on the engine feet (blue) plotted together the spectrum of the vibrations received on the engine foundation (red).

It can be seen that the fire orders are less strong and disappearing with increasing frequency. In Figure 20 shows the ship structure vibration. Engine induced acceleration is less strong due to the resilient mounting system. Mainly, structure excitation forces are appearing at propeller harmonics.

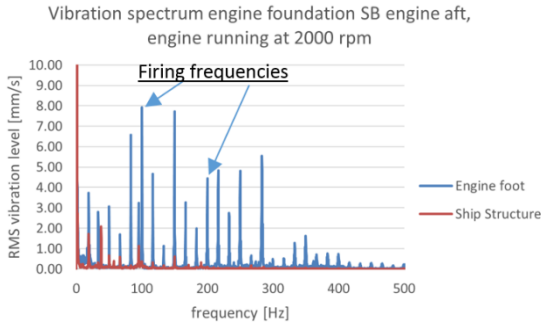

Figure 19 Vibration meaurements on the engine foot at 2000rpm

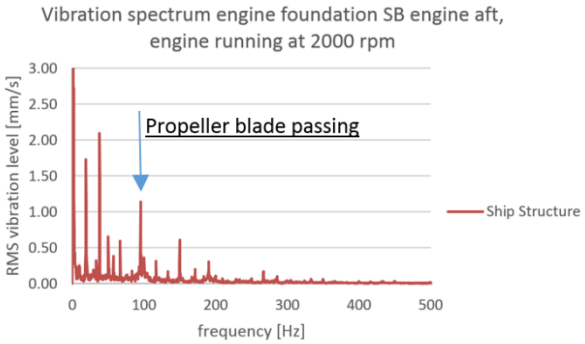

Figure 20 Vibration meaurements on the ship structure at 2000rpm

4. CONCLUSIONS

This paper presents off-board and on-board measurements of the Princess Royal associated with cavitation. Still pictures above the propellers shown to describe the types of cavitation.

Measurements were taken for a various CPA distance and operation speed. Most of the data could not be presented due to the dominating self-noise of the supply vessel and the hydrophone array.

A SL calculation model depends on environmental conditions, frequency range, source and hydrophone locations. That make the model very complicated and it also may cause uncertainty. The SL of the vessel calculated by taking into account transmission loss, free surface (Lloyd's mirror effect) as well as bathymetry and sediment of the seabed (bottom reflection loss) due to the (acoustically) shallow water condition of the trial location.

The SL graph shows the URN level increasing with speed of the vessel. Dominant peaks can be detected at the main engine and the propellers harmonics. It could be problematic to determine main source of the PR without the support of the pressure pulse and vibration measurements due to the firing and blade passing frequencies are very close. The URN contribution from the

diesel engines is not significant since efficient isolating performance of the flexible mountings that is confirmed through the vibration measurements.

ACKNOWLEDGMENTS

The research, basis for the study made in preparation of this paper, has been supported by the European Union 7th Framework Programme (FP7) project SONIC under grant agreement No: 314394.

REFERENCES

Ainslie, Michael A. (2010). Principles of sonar performance modelling, Springer.

ANSI (2009), Quantities and Procedures for Description and Measurement of Underwater Sound from Ships – Part 1: General Requirements, ANSI/ASA S12.64, American National Standards Institute, New York

Atlar, M., Aktas, B., Sampson, R., Seo, K. C., Viola, I. M., Fitzsimmons, P. & Fetherstonhaugh, C. (2013). 'A Multi-purpose marine science & technology research vessel for full-scale observations and measurements'. AMT'13, Gdansk.

Atlar, M., Takinaci, A., C., Korkut, E., Sasaki, N. & Aono, T. (2001). 'Cavitation tunnel tests for propeller noise of a FRV and comparisons with full-scale measurements'. http://resolver. caltech. edu/cav2001: sessionB8. 007.

Brekhovskikh, Leonid Maksimovich (2003). Fundamentals of ocean acoustics, Springer Science & Business Media.

Codarin, Antonio, Wysocki, Lidia E., Ladich, Friedrich & Picciulin, Marta (2009). 'Effects of ambient and boat noise on hearing and communication in three fish species living in a marine protected area (Miramare, Italy)'. Marine Pollution Bulletin 58(12): 1880-1887.

ISO/PAS 17028-1: 2012. "Acoustics — Quantities and procedures for description and measurement of underwater sound from ships Part 1: General requirements for measurements in deep water", ISO, Geneva.

Nilsson, S. & Tyvand, N. P. (1981). Noise Sources in Ships: I Propellers, II Diesel Engines, Nordic Cooperative Project: Structure Borne Sound in Ships from Propellers and Diesel Engines, Nordforsk, Norway.

Noise, Ocean (2003). 'Marine Mammals National Academies Press Washington'. DC 1: 220.

Richardson, W. J., Greene Jr, C. R., Malme, C. I. & Thomas, D. H. (1995). Mammals and noise, San Diego: Academic Press.

Ross, Donald (1976). Mechanics of underwater noise, DTIC Document.

Sampson, R., Turkmen, S., Aktas, B., Shi, W., Fitzsimmons, P. & Atlar, M. (2015). 'On the full scale and model scale cavitation comparisons of a Deep-V catamaran research vessel'. Proceedings of 4th International Symposium on Marine Propulsors (SMP'15), Austin, Texas. June.

Schuiling, Bart, Lafeber, Frans Hendrik, van der Ploeg, Auke & van Wijngaarden, Erik (2011). 'The influence of the wake scale effect on the prediction of hull pressures due to cavitating propellers'. Second International Symposium on Marine Propulsors SMP.

Slabbekoorn, Hans, Bouton, Niels, van Opzeeland, Ilse, Coers, Aukje, ten Cate, Carel & Popper, Arthur N. (2010). 'A noisy spring: the impact of globally rising underwater sound levels on fish'. Trends in ecology & evolution 25(7): 419-427.

SONIC. (2012). "Suppression Of underwater Noise Induced by Cavitation." Retrieved 10 March 2017, from http://www.sonic-project.eu/.

Turkmen, S., Aktas, B., Atlar, M., Sasaki, N., Sampson, R. & Shi, W. (2017). 'On-board measurement techniques to quantify underwater radiated noise level'. Ocean Engineering 130: 166-175.

Urick, Robert J. (1967). Principles of underwater sound for engineers, Tata McGraw-Hill Education.

Van, W. & Hendrik, C. (2011). 'Prediction of propeller-induced hull-pressure fluctuations'.

Zoet, P., Turkmen, S., Kellett, K., Aktas, B., Sampson, R., Shi, W., Atlar, M., & Turan, O., (2015) "On-board structure borne noise measurements and underwater radiated noise," 4th International conference on advanced model measurement technology for the maritime industry (ATM'15) , September, Istanbul.

DISCUSSION

Question from Sverre Steen

Can you say something about the constancy and repeatability of your measurement?

Did you perform any repeated measurements?

Author's closure

Yes, repeated measurements were performed. Every operation condition, in terms of main engine speed, was run twice for each closest point to approach (CPA) distance. For instance, the graph below show the constancy and repeatability of received level at engine speed 2000rpm. The noise spectrums show a similar trend at each run. Some of the results of the measurements didn't show

this similarity mainly because of the self-noise of the measurement equipment.

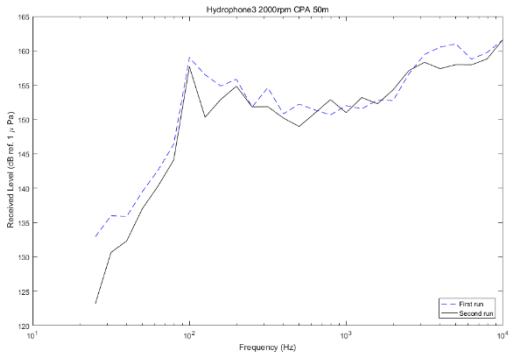

Figure A1 Comparison of first and second run of the received level noise spectrum at 1200rpm

Question form Johan Bosschers

Did you compare your shallow water source level with deep water source level measurements performed in the past?

Author's closure

Yes, comparisons of source level were made between measurements taken in 2013 when the target vessel was operated in deep water (100 m), and measurements taken in 2014 when the target vessel was operated in shallow water (17 m). In the graph below the received level noise spectrum, measured in 2013 and 2014, is presented at engine speed 2000 rpm

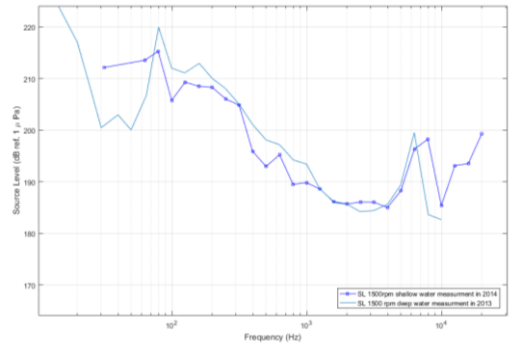

Figure A2 Comparison of first and second run of the received level noise spectrum at 1200rpm

Question from R CH Lenng

Use of hydrophones away and beamforming technique can minimize the surface and bottom reflections problem.

Author's closure

Yes, the beamforming method could be performed to determine the noise contributions from different noise sources at different angles.In this study, noise sources were identified by combining vibration measurements with the URN data in a narrowband.

Theoretically calculated the Lloyd's Mirror Interface Pattern and sea bottom loss were used to establish the noise contribution of reflected sound from the free surface and seabed.